

Development of Efficient Interface Sharpening Procedure for Viscous Incompressible Flows

Arnas KAČENIAUSKAS

Laboratory of Parallel Computing, Vilnius Gediminas Technical University
Sauletekio al. 11, 10223 Vilnius, Lithuania
e-mail: arnka@fm.vtu.lt

Received: November 2007; accepted: April 2008

Abstract. The paper describes the development of the efficient interface sharpening procedure for viscous incompressible flows governed by the Navier–Stokes equations. The moving interface has been captured by a pseudo-concentration method. The solution domain has been discretised by the space-time finite elements, while numerical schemes have been stabilised by the Galerkin least squares method. The dam break problem including breaking waves has been solved in order to validate the performance of the numerical technique. The computed position of the leading edge of water column has been compared with the experimental measurements. The detailed investigation of numerical parameters governing the sharpness of the front and mass conservation has been presented.

Keywords: moving interfaces, interface sharpening procedure, the pseudo-concentration method, the finite element method, dam break problem, breaking waves phenomena.

1. Introduction

Many important industrial applications of viscous incompressible flows involve propagation of moving interfaces. Numerous examples include actual problems such as coating process, ship in waves analysis, melting and solidification, crystal growth, nuclear fusion, metal forming, tank sloshing and dam break. Numerical simulation of moving interface flows presents great challenges to computational scientists, because the underlying physical problem is sensitive to small numerical perturbations. The developed software has to identify the unknown interface, to follow its kinematics and to resolve a strong coupling between the interface propagation and dynamics of the continuum.

Numerical methods developed for solving moving interface problems might be classified into two categories: interface tracking techniques (ITT) and interface capturing techniques (ICT). In the first category of interface simulating methods, a moving interface is represented and tracked explicitly either by making it with special marker points, or by attaching it to a mesh surface. The earliest works (Hirt *et al.*, 1970) were based on the Lagrangian description of motion. A mesh deforms severely as a free surface moves, making remeshing and rezoning necessary at each time step (Radovitzky and Ortiz, 1998). In the Arbitrary Lagrange-Eulerian approach (Hirt *et al.*, 1974), a mesh

deforms in terms of an arbitrary velocity field, which is independent of the flow velocities, except at the moving interface. Various ITT (Masud and Hughes, 1997; Del Pin *et al.*, 2007) for attaching the interface to a mesh surface were developed during the past decades using the finite element method (FEM). The ITT based on the Lagrangian approach or the Arbitrary Lagrange-Eulerian approach use moving unstructured meshes, allowing us to employ the full power and flexibility of the FEM. However, these methods are unable to cope naturally with interface interacting with itself by folding or rupturing. Only at a cost of complex implementation they simulate the discussed phenomena.

In the second category of interface simulating methods, either massless particles or an indicator function marks gas or fluid on either side of the interface. The ICT require no geometry manipulations after the mesh is generated and can be applied to interfaces of a complex topology. The marker-and-cell method (Harlow and Welch, 1965), the volume of fluid method (Hirt and Nichols, 1981) and the level set method (Osher and Sethian, 1988) are well known methods using the ICT idea and the Eulerian approach. The volume of fluid method is very efficient and practical (Mencinger and Žun, 2007), therefore, it is implemented in a lot of commercial codes using the finite volumes. However, the location of the interface is not explicit and, sometimes, the appropriate boundary conditions cannot be prescribed with a required accuracy. The application of the continuum surface force model (Brackbill *et al.*, 1992) can resolve this complicated problem only partially.

The level set method is based on finite difference schemes. The mathematical model of the level set method is very universal. This method automatically takes care of merging and breaking of the interface, therefore, it is capable of simulating interfaces that undergo large topological changes. The bottleneck of such interface capturing techniques as the level set method is excessive numerical diffusion which smears the sharpness of the moving front. The level set function is initially a distance function, but this property does not hold after several time steps. If the level set function is not re-initialized, areas of small and large gradients change the thickness of the interface. It was also observed that numerical diffusion introduces a normal motion proportional to the local curvature of the interface, which leads to significant difficulties in preserving mass conservation. A lot of re-initialization procedures (Sussman and Fatemi, 1999) were introduced to remedy the undesirable effects, but their numerical implementation is quite complicated and requires large computational resources. The first publications presenting attempts to combine the level set method and finite elements appeared in the past decade (Kačeniauskas, 2000; Quecedo and Pastor, 2001; Nagrath *et al.*, 2005; Grooss and Hesthaven, 2006).

A pseudo-concentration method (Thompson, 1986) often used with the FEM is interesting alternative for the level set method. This method uses a pseudo-concentration function defined in the entire domain and solves a hyperbolic equation to determine the moving interface. The choice of function features depends on different numerical schemes employed in the solution procedure by different authors (Nakayama and Shibata, 1998; Lewis and Ravindran, 2000). In the most cases, the pseudo-concentration method is more efficient than the level set method, because it uses simpler front reconstruction techniques. The FEM has become a powerful tool for solving many scientific and engineering applications, therefore, the demand for further investigation of the ICT and implementation in commercial FEM codes is rapidly growing (Tezduyar, 2007).

One of the concerns with the ICT has been sustaining the interface sharpness and global mass conservation in long-time integrations. The function defining the interface undergoes some diffusion as it is advected through the computational domain. It leads to interface smearing and non-physical mass transfer between the two fluids. Re-initialization procedures proposed within the framework of the level set method are based on the numerical solution of the non-linear PDE on the whole solution domain or its part (Sussman and Fatemi, 1999). The re-initialization may need more computational resources than the whole flow solver (Kačeniauskas, 2000). The interface sharpening techniques (Aliabadi and Tezduyar, 2000) employed together with the pseudo-concentration method include various numerical parameters, which values might depend on the mesh size, the time step and the physics of the flow. Thus, the choice of the numerical schema, the interface sharpening procedure and numerical parameters remains state of the art problem.

In the present paper, the efficient interface sharpening procedure is developed examining the influence of particular numerical parameters to the complex dam break flow. An outline of the paper is as follows. Section 2 describes a mathematical model of the considered flow. Section 3 presents the developed interface sharpening procedure. Numerical results and the values of governing numerical parameters are discussed in Section 4. Conclusions are given in Section 5.

2. Mathematical Model of the Flow

The laminar and Newtonian flow of viscous and incompressible fluids is described by the Navier–Stokes equations in the Eulerian reference frame:

$$\rho \left(\frac{\partial u_i}{\partial t} + u_j \frac{\partial u_i}{\partial x_j} \right) = \rho F_i + \frac{\partial \sigma_{ij}}{\partial x_j}, \quad (1)$$

$$\frac{\partial u_i}{\partial x_i} = 0, \quad (2)$$

where u_i are the velocity components; ρ is the density; F_i are the gravity force components and σ_{ij} is stress tensor:

$$\sigma_{ij} = -p\delta_{ij} + \mu \left(\frac{\partial u_i}{\partial x_j} + \frac{\partial u_j}{\partial x_i} \right), \quad (3)$$

where μ is dynamic viscosity coefficient; p is pressure and δ_{ij} is Kronecker delta. Slip boundary conditions for velocity are prescribed on rigid walls:

$$u_i n_i = 0, \quad (4)$$

where n_i are components of a unit normal vector. This is usual choice of boundary conditions used for modelling of moving interface flows. The zero stress boundary conditions

are prescribed on the open upper boundary:

$$\sigma_{ij}n_j = 0. \quad (5)$$

The reference pressure is prescribed on the upper wall. The zero initial conditions are prescribed for the Eqs. (1)–(3) in the performed investigation.

The pseudo-concentration method (Thompson, 1986) is developed for moving interface flows using the Eulerian approach and the interface capturing idea. The pseudo-concentration function φ serves as a marker, identifying fluids A and B with densities ρ_A and ρ_B and viscosities μ_A and μ_B . In this context, the density and viscosity are defined as

$$\rho = \varphi\rho_A + (1 - \varphi)\rho_B, \quad (6)$$

$$\mu = \varphi\mu_A + (1 - \varphi)\mu_B, \quad (7)$$

while $\varphi = 1$ for fluid A and $\varphi = 0$ for fluid B. The evolution of the interface is governed by a time dependent convection equation

$$\frac{\partial\varphi}{\partial t} + u_j \frac{\partial\varphi}{\partial x_j} = 0. \quad (8)$$

The velocity u_j is obtained from the solution of the Navier–Stokes equations (1)–(3). The initial conditions defined on the entire solution domain should be prescribed for the (8).

The space-time Galerkin least squares (GLS) finite element method (Masud and Hughes, 1997) is applied as a general-purpose computational approach to solve the partial differential equations (1)–(3), (8) with boundary conditions (4)–(5) applied. Equal order bilinear shape functions are used for both the pressure and velocity components as well as for the pseudo-concentration function. The stabilization nature of the formulation prevents numerical oscillation of incompressible flows when equal-order interpolation functions for velocity and pressure are used and preserves the consistency of the standard Galerkin method when adaptive remeshing is performed. The detailed description of variational formulation and stabilization parameters can be found in the work (Kačeniauskas and Rutschmann, 2004).

3. Interface Sharpening Procedure

The standard Galerkin formulation of the FEM yields oscillatory solutions when applied to convection dominant problems in conjunction with classical time stepping algorithms. Conventional stabilization techniques add to the (8) artificial viscosity terms, introducing numerical diffusion and reducing numerical oscillations. In practical application of the GLS stabilizing method to the complex problems governed by convective transport, some overshoots and undershoots are observed (Kačeniauskas, 2004). In order to apply the developed interface sharpening procedure, a simpler limiter should be implemented:

$$\varphi = \min [\max[\varphi^{old}, 0], 1]. \quad (9)$$

It removes the overshoots and undershoots, preventing the numerical technique from unexpected incorrect values and the loss of accuracy.

While the (8) moves the interface at a correct velocity, the pseudo-concentration function may become significantly influenced by the numerical diffusion after some period of time. It leads to interface smearing and problems with mass conservation. The pseudo-concentration function should be reconstructed in order to maintain interface sharpness. In this work, the investigated interface sharpening procedure is similar to that proposed in the article (Aliabadi and Tezduyar, 2000). The values of the pseudo-concentration function φ are replaced by the values of the reconstructed function ϕ , considering the following formula:

$$\phi = c^{1-a}\varphi^a, \quad 0 \leq \varphi \leq c, \quad (10)$$

$$\phi = 1 - (1 - c)^{1-a}(1 - \varphi)^a, \quad c \leq \varphi \leq 1, \quad (11)$$

where the parameter c represents mass conservation level, while a governs sharpness of the moving interface. Fig. 1 illustrates the interface sharpening procedure for 1D case. The curve F is smooth φ function, while other curves a20c05, a11c05, a15c07 are sharpened by using sets of parameters $a = 2.0$ and $c = 0.5$, $a = 1.1$ and $c = 0.5$, $a = 1.5$ and $c = 0.7$, respectively. The curves a20c05 and a11c05 illustrate the interface sharpening, while the curve a15c07 shows mass correction combined with the interface sharpening. The implicit parameter ns indicates how often this procedure should be applied. Usually, the interface thickness tends to grow, occupying a wide band of finite elements (Fig. 2a). Frequent application of the interface sharpening procedure (10)–(11) with large a values easily resolves this problem, but it can distort the smoothness of the interface (Fig. 2c). The moving front can adapt to the FE mesh proceeding “staircases”. In this undesirable case, the accuracy of the ICT becomes directly limited by the mesh size. Thus, the values of parameters a and ns , controlling interface sharpness, should be considered very carefully.

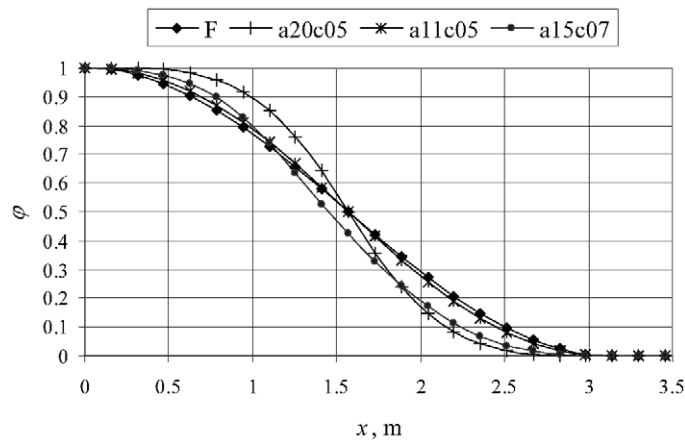


Fig. 1. Illustration of the interface sharpening procedure.

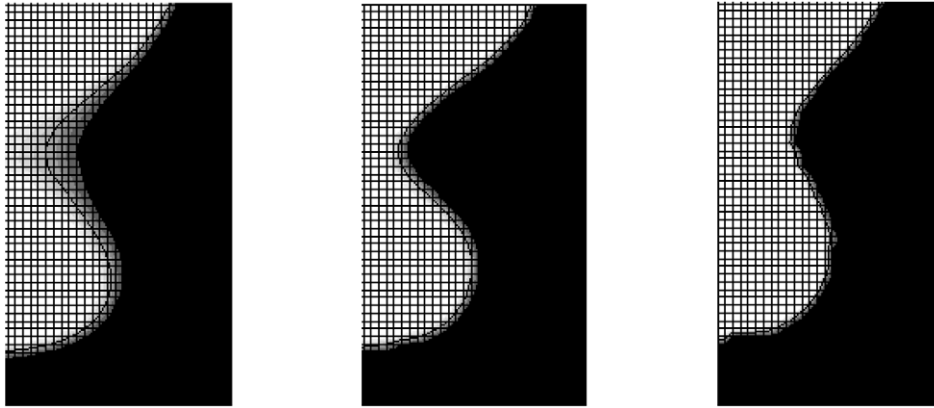


Fig. 2. Illustration of the maximum interface thickness: (a) 8 elements, no sharpening, (b) 2 elements, $ns = 10$, $a = 1.5$, (c) 1 element, $ns = 5$, $a = 1.9$.

Mass conservation is a very important issue of the interface sharpening algorithm. Insignificant numerical errors which result in slight non-physical mass transfer between the two fluids may lead to significant errors in long-term time integration of the problem. In order to overcome this difficulty, the values of coefficient c should be computed considering precise mass distribution in the interface region. At any time, mass conservation for fluid A can be described by the formula

$$M_A = \rho_A \int_{\Omega} \phi \, d\Omega, \quad (12)$$

where M_A is the initial mass of the fluid A. The equation for determining c can be obtained by substituting ϕ from formulas (10)–(11) to (12). Assuming that a is given and constant, the resulting equation can be written as follows:

$$K_1 c^{1-a} - K_2 (1-c)^{1-a} = M_A - M_A^\varphi, \quad (13)$$

where coefficient K_1 is defined on the narrow band of the moving interface:

$$K_1 = \rho_A \int_{\Omega} \varphi^a \, d\Omega, \quad 0 \leq \varphi \leq c. \quad (14)$$

Coefficient K_2 is computed on the remaining part of the interface:

$$K_2 = \rho_A \int_{\Omega} (1-\varphi)^a \, d\Omega, \quad M_A^\varphi = \rho_A \int_{\Omega} \varphi \, d\Omega, \quad c \leq \varphi \leq 1. \quad (15)$$

Coefficient M_A^φ represents the current mass of the fluid A, defined by the values of function φ . The right side of (13) means mass deviation from the initial mass M_A . Despite the fact that only one fluid is explicitly presented in Eqs. (12)–(15), the described procedure conserves mass for each fluid. In the solved problems, the fluid A is heavy (water),

while the fluid B is relatively light (air). Mass correction applied to the heavier fluid A helps to ensure maximal accuracy of the procedure. A good starting value for c is 0.5, which indicates satisfactory mass conservation. The final values of c are obtained solving one-dimensional non-linear (13). It can be solved by different iterative methods. The numerical tests performed show good convergence for the investigated problem, therefore, the detailed convergence study and the implementation procedure are not presented in this text. However, modelling breaking waves and other extreme phenomena, the final c values vary in a relatively wide range from 0.2 to 0.8. After determining a and c , the Eqs. (10)–(11) are satisfied at the node-level, and the new value of the pseudo-concentration function is used to resume computations.

4. Numerical Results and Discussions

The discussed numerical algorithms have been implemented in the code FEMTOOL (Kačeniauskas and Rutschmann, 2004), which allows implementation of any partial differential equation with minor expenses. Time dependent problems are solved using space-time finite elements. The order of shape functions is determined by input and is limited neither in space nor in time. A given transient problem can be solved in several implicit time steps from one time level to the other or in one single implicit step for all time levels. Space-time finite element integration in time and the high order shape functions generated automatically make FEMTOOL to be applicable to complex strongly coupled problems of interest. Benchmark tests have been performed on the PC cluster VILKAS of Vilnius Gediminas Technical University and on the LitGRID clusters (<http://www.litgrid.lt/>).

4.1. Description of a Dam Break Problem

The developed interface sharpening procedure has been applied for modelling a dam break flow, which has been the subject of extensive research for a long time (Martin and Moyce, 1952). The breaking wave phenomena, occurring in some cases of a dam break problem, includes it into the class of complex applications such as solitary wave propagation, tank sloshing and water on a ship deck simulation. Some experimental measurements were performed on the dam break flow. Photographs showing the time evolution of the collapsing column as well as the wave returning after hitting a wall on the opposite side (Koshizuka *et al.*, 1995) are available for the purpose of evaluating the numerical methodology on the basis of flow visualization. Measurements of the exact interface shape are not available, but some secondary data such as the reduction of the water column height can be employed for quantitative comparison of the obtained results (Martin and Moyce, 1952). Several modifications of the broken dam problem have been extensively used as classical test cases for numerical simulation of free surfaces and moving interfaces (Hirt and Nichols, 1981; Soulis, 1992; Quecedo *et al.*, 2005). However, the universal, accurate and efficient numerical technique for breaking wave simulation attracts big attention of research community and software developers.

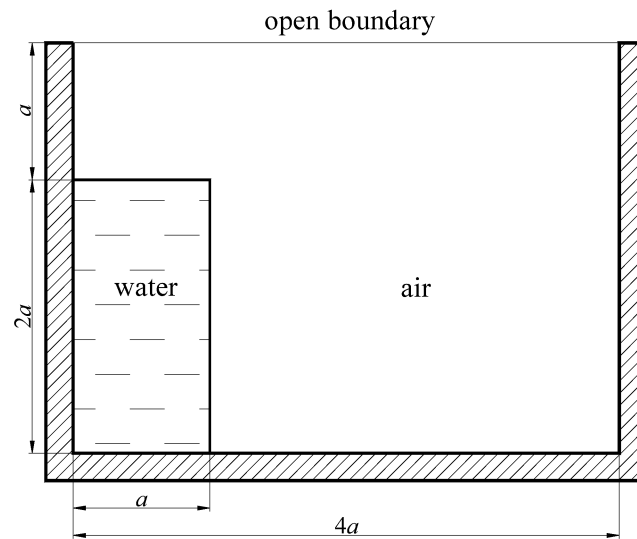


Fig. 3. Geometry of the dam break problem.

The geometry of the solution domain is shown in Fig. 3. The dimensions of the reservoir and the water column correspond to those used in the experiment carried out by Koshizuka *et. al.* The reservoir is made of glass, with a base length of 0.584m. The water column, with a base length of 0.146m and the height of 0.292m ($a = 0.146\text{m}$), was initially supported on the right by a vertical plate drawn up rapidly at time $t = 0.0\text{s}$. The water falls by gravity ($g = 9.81\text{m/s}^2$), acting vertically downwards. The density of water is $\rho_A = 1000\text{kg/m}^3$, while the dynamic viscosity coefficient is $\mu_A = 0.01\text{kg/(m}\cdot\text{s)}$. The density of air is taken to be $\rho_B = 1\text{kg/m}^3$, and the dynamic viscosity coefficient is $\mu_B = 0.0001\text{kg/(m}\cdot\text{s)}$. The slip boundary conditions (4) are applied to the bottom and sides of the reservoir. The stress boundary conditions (5) are prescribed on the upper open boundary. They may be changed to fixed pressure and zero normal gradients of the velocities. The computations are performed on the structured finite element meshes of different resolution – 120×90 and 240×180 . The investigated time interval is $t = [0.0; 1.0]\text{s}$. The size of the time step is $\Delta t = 0.001667$ for the 120×90 finite element mesh. The number of time steps is equal to 600. The size of the time step for the 240×180 finite element mesh is $\Delta t = 0.000667$. The number of the time steps used is equal to 1500.

4.2. Breaking Wave Phenomena and Validation of Numerical Results

Fig. 4 illustrates the breaking wave phenomena simulated by the pseudo-concentration method and the developed interface sharpening technique. The pseudo-concentration function value 0.5 represents the exact shape of moving interface. Grey colours show the transition region between different fluids. Gravity causes the water column on the left of the reservoir to seek the lowest possible level of potential energy. Thus, the column will collapse and eventually come to rest. The initial stages of the flow are dominated by

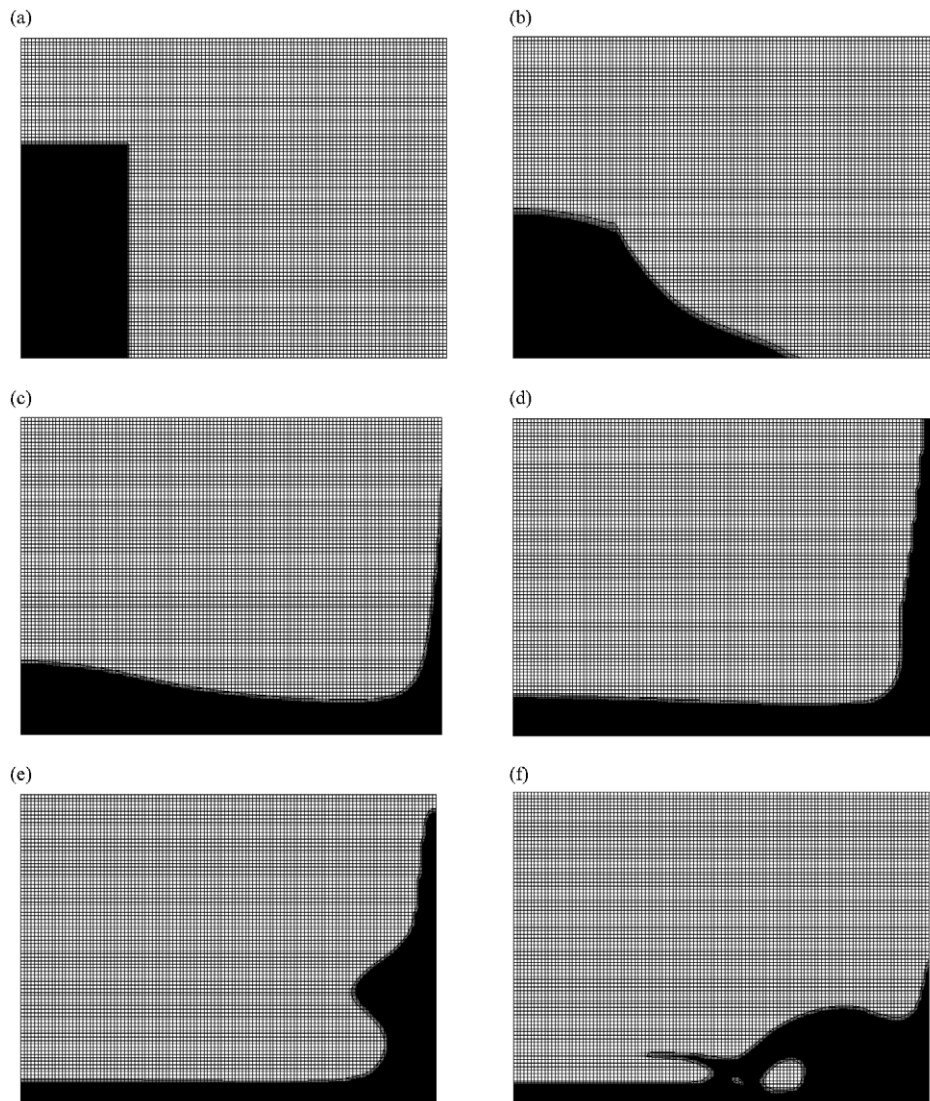


Fig. 4. The dam break flow visualization by the pseudo-concentration function on the stationary finite element mesh: (a) $t = 0.0s$, (b) $t = 0.1666s$, (c) $t = 0.3333s$, (d) $t = 0.5s$, (e) $t = 0.6666s$, (f) $t = 0.8333s$.

inertia forces with viscous effects increasing as the water comes to rest. On such a large scale, the effect of surface tension forces is insignificant. When $t = 0.36s$, water tends to leave the computational domain. The appropriate boundary conditions could handle this phenomenon. The natural mass loss is observed for the period of time approximately equal to $0.24s$. This leads to additional difficulties in global mass conservation for the whole simulation time. The additional boundary conditions for φ are implemented on the

upper boundary, which sometimes could be treated as inflow:

$$\varphi = 0 \text{ if } u_i n_i < 0. \quad (16)$$

The boundary conditions (16) are applied, when the computed current mass becomes very close to initial mass, which indicates that the lost water has come back to the computational domain. The implemented technique helps to simulate the fluid A, leaving and entering the computational domain. The complexity of velocity fields, occurring at different stages of breaking wave phenomena, can be easily captured using simple structured meshes. To predict the behaviour of the small bubbles correctly is a more difficult task. When $t = 0.83\text{s}$, the backward moving wave has folded over and a small amount of air is trapped. However, in experiments, this air is present in the form of small bubbles. The current methodology has been derived for sharp interfaces, therefore, the mesh needs significant refinement to a resolution smaller than the bubble size.

The numerical results have been validated by the quantitative comparison with experimental measurements obtained for the early stages of this experiment (Martin and Moyce, 1952; Koshizuka *et al.*, 1995). Non-dimensional position of the leading edge of the collapsing water column on the left wall versus non-dimensional time is shown in Fig. 5. Non-dimensional time t^* is defined by the formula

$$t^* = t\sqrt{2g/a}. \quad (17)$$

Two different sets of experimental data E1 and E2 were presented by Martin and Moyce, illustrating the difficulty to determine the exact position of the leading edge. A thin layer of water shoots over the bottom and the rest of the bulk flow follows behind it. The initial numerical experiments have overestimated the position of the leading edge. Almost identical values have been obtained by using two structured finite element meshes

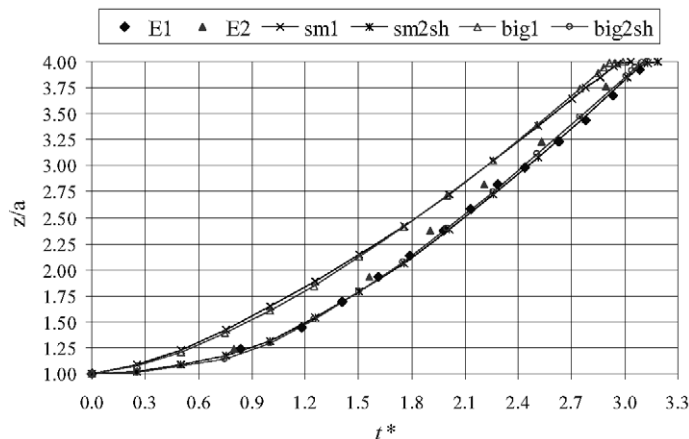


Fig. 5. Quantitative comparison of the numerical results and experimental measurements (E1, E2). Non-dimensional position of the leading edge z/a versus non-dimensional time t^* .

of different resolution, 120×90 and 240×180 (the curve sm1 and the curve big1, respectively). The curve sm1 has been computed by using the interface sharpening parameters $ns = 5$ and $a = 1.5$. The curve big1 has been computed by using the interface sharpening parameters $ns = 20/Cu$ and $a = 1.3$. The numerical results have been improved postponing the thin liquid layer by intensive sharpening of the moving interface. Low values of the pseudo-concentration function have been filtered by the interface sharpening at each time step with high a values. The curves sm2sh and big2sh have been computed by using $ns = 1$, $a = 2.0$. The numerical experiments have shown that the extreme sharpening is necessary only at the beginning of the time interval $t = [0; 0.09]$ s. Thus, the accuracy of the obtained results is strongly influenced by the numerical parameters, but it is almost independent of the resolution of the finite element mesh, if sufficiently dense FE meshes are used.

4.3. The Interface Sharpness

The quantitative comparison of the numerical results and the experimental measurements has shown that the detailed analysis of the interface sharpening parameters should be performed in order to develop an accurate and efficient interface sharpening procedure. The sharpening frequency ns determines how often the interface sharpening procedure should be applied. Initially, interface sharpening has been performed at regular time intervals (each k time step). Fig. 6a shows time evolution of the total number of nodes $totnum$, belonging to the interface ($0 < \varphi < 1$). The value of parameter a is fixed and equal to 1.5. The curve nsk0 illustrates how the interface grows without sharpening. It is obvious that this process is drastically influenced by the numerical diffusion. On the contrary, the interface sharpening performed at each time step reduces the interface thickness to one finite element (the curve nsk1). However, in this case, the moving interface loses its smoothness (Fig. 2c). The results obtained in sharpening the interface less frequently are quite acceptable. The case $ns = 5$ is illustrated by the curve nsk5. The curve nsk10 visualizes the case $ns = 10$.

Fig. 6b illustrates the influence of the parameter a on the total number of the interface nodes. The sharpening frequency ns is fixed and equal to 5. Various values of a have been

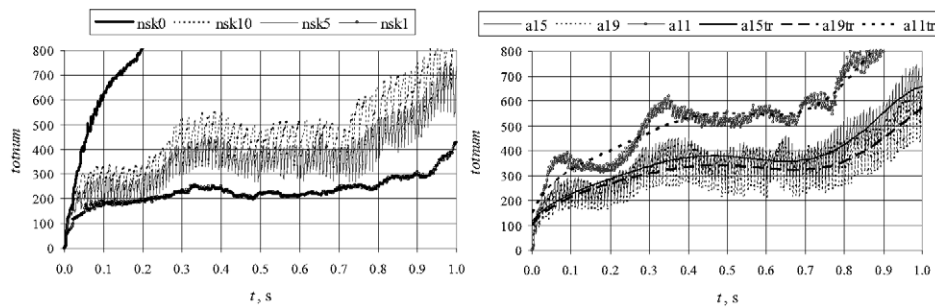


Fig. 6. Time evolution of the total number of the interface nodes $totnum$: (a) the influence of the parameter ns , (b) the influence of the parameter a .

investigated, but only particular curves are shown in this figure. The application of the interface sharpening procedure is not efficient in the case of $a = 1.1$ (the curve a11). The decrease of the number of interface nodes is not significant. The improvement obtained by using higher a values is not very large for the investigated sharpening frequency. The difference between the curves a15 ($a = 1.5$) and a19 ($a = 1.9$) is quite small. The plotted trend lines (a11tr, a15tr, a19tr), based on the sixth order polynomials, clearly illustrate this issue. The values higher than 2.0 distort the interface smoothness, therefore, they can be applied only in special cases for short time intervals. The shape of the interface is very complicated and not known a priori. The length of the interface always changes, therefore, it is difficult to compute its actual thickness either analytically or numerically.

In this work, the frequency of the interface sharpening is defined by a simple indicator, based on the Courant number

$$ns = \text{int}\left(\frac{k}{Cu}\right), \quad Cu = |v| \frac{\Delta t}{\Delta x}, \quad (18)$$

where Cu is the maximum Courant number, k is a coefficient, Δt is the time step, Δx is the mesh size, $|v|$ is a measure of maximum velocity. In general, the frequency of the interface sharpening might depend on the time step, the mesh size and the flow. Thus, the most important parameters are considered in the formula (18). If $Cu < 1$, the interface cannot cross the whole finite element during this time step. Therefore, there is no need to sharpen it more frequently than $\text{int}(1/Cu)$. Fig. 7 shows time evolution of the total number of the interface nodes obtained while sharpening the interface at every 10 time steps (the curve nsk10) and applying the indicator with $k = 10$ (the curve cuk10). The trend lines (nsk10tr and cuk10tr), based on the sixth order polynomials, illustrate quantitatively similar results, despite the different character of the interface sharpening. Other indicators evaluating the relative interface thickness have also been investigated.

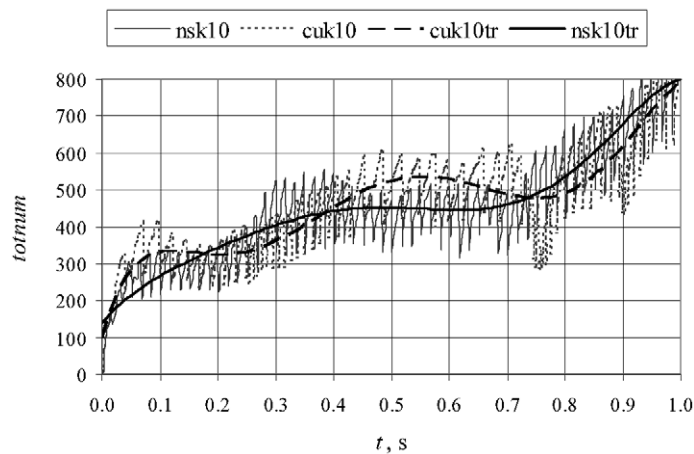


Fig. 7. Time evolution of the total number of the interface nodes *totnum*: the curve nsk10 is obtained by using regular interface sharpening $ns = 10$, the curve cuk10 is obtained by using the indicator $ns = 10/Cu$.

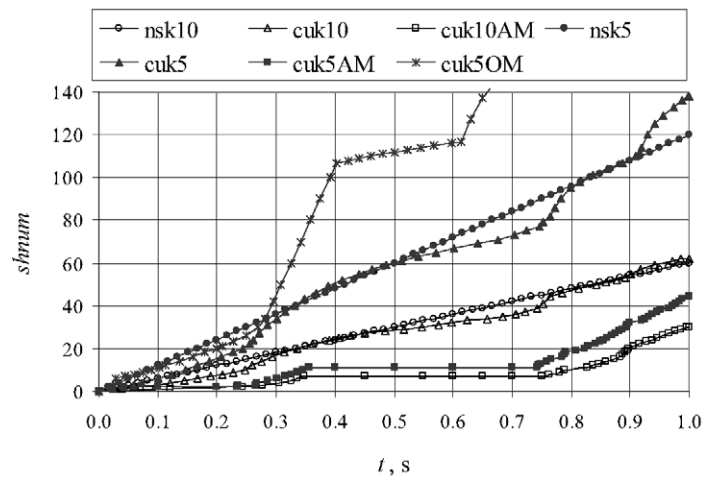


Fig. 8. Time evolution of the interface sharpening number $shnum$.

The ratio between the number of nodes, where φ is close to unity or zero, and the variable $totnum$ has been computed. The stochastic character of the obtained curves has not allowed the information provided by these indicators to be efficiently exploited, therefore, the detailed investigation is not presented in this work.

The developed interface sharpening procedure is very efficient. There is no need to solve any PDE numerically (Čiegis and Starikovičius, 2003; Maknickas *et al.*, 2006) on the whole solution domain or its part (Sussman and Fatemi, 1999). The time-consuming geometrical techniques for interface reconstruction has not been applied either. Formulas (10)–(11) are satisfied at the node level and can be implemented as any post-processing of the numerical solution of the (8). In order to preserve mass conservation, the non-linear one-dimensional (13) should be solved. The computation of the coefficients defined by formulas (14)–(15) is more time consuming, but it can be implemented by using additional conditional statements in the procedure devoted for the global mass calculation. The interface sharpening procedure is not applied at every time step, therefore, the interface sharpening number $shnum$ can be treated as the relative efficiency measure. Fig. 8 illustrates time evolution of the interface sharpening number $shnum$ for different strategies. The interface sharpening produced at regular time intervals (the curves $nsk5$ and $nsk10$) and that (the curves $cuk5$ and $cuk10$) defined by the formula (18) give very similar quantitative efficiency results. Other curves ($cuk5AM$, $cuk5OM$ and $cuk10AM$) illustrate the attempts to improve the sharpening quality by evaluating the needs of mass conservation.

4.4. Mass Correction

Mass conservation is one of the most important tasks for any interface sharpening procedure. Sometimes, interface handling can be related to the unwanted instabilities caused by large density ratios. This is due to the discontinuous density at the interface. In this work,

density smoothing is performed carefully computing its values in the finite element *area*. The density is taken to be constant in the finite element and φ values in the formula (6) are averaged:

$$\varphi_{EL} = \frac{\sum_{i=1}^n G_i \varphi_i}{area}, \quad (19)$$

where n is the number of Gauss points; G_i are Gauss coefficients; φ_i are the values of the pseudo-concentration function φ at Gauss points. The strategy implemented by using the formula (19) works very well when the interface is not very sharp and its thickness is greater than the size of an element. On the contrary, the global mass computations are performed evaluating the non-smoothed density (equal to 1kg/m^3 or 1000kg/m^3) at the Gauss points:

$$M_{EL} = \sum_{i=1}^n G_i \rho_i, \quad (20)$$

where M_{EL} is the fluid mass in the finite element *EL*; ρ_i denotes the density values at Gauss points. Formula (20) yields higher accuracy and higher oscillations of the global mass curves as well.

Fig. 9 shows mass evolution in time for several interface sharpening cases. The time interval $t = [0.4; 0.7]\text{s}$ illustrates the case when water is leaving the computational domain and is coming back. In order to preserve the consistency between the flow physics and the numerical techniques, mass correction is automatically switched off in this special case. All plotted curves are actually of the same character, but quantitative results are quite different. The significant mass loss is observed when interface sharpening is not applied (the curve *nsk0*). The interface sharpening without mass correction at regular time intervals (the curve *nsk10*, $ns = 10$) does not significantly reduce the mass loss. The

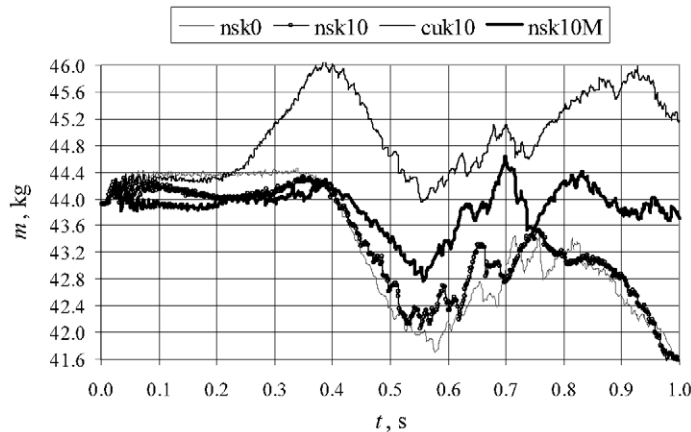


Fig. 9. Time evolution of the global mass for different strategies of interface sharpening.

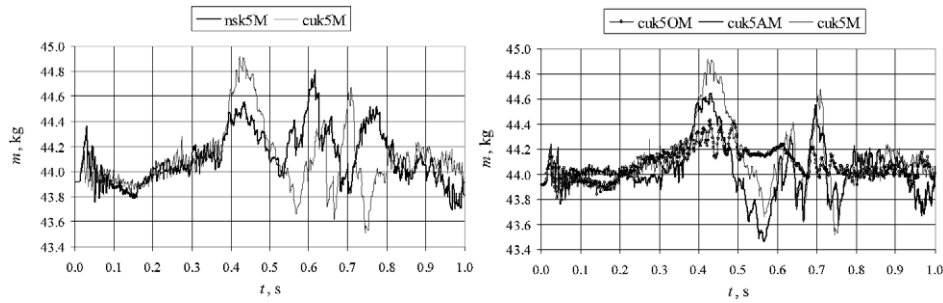


Fig. 10. The global mass conservation in time: (a) the interface sharpening governed only by the ns values, (b) the interface sharpening additionally handled by the mass error.

adaptation of the interface sharpening frequency to Cu number changes the character of the numerical solution (the curve $cuk10$, $k = 10$). However, mass becomes overestimated. Only the application of mass correction to regular interface sharpening (the curve $nsk10M$, $ns = 10$) significantly improves mass conservation.

Mass corrections combined with interface sharpening can be applied in several different ways. Fig. 10 illustrates the issues of interface sharpening additionally handled by the mass error. The curves $nsk5M$ and $cuk5M$ are obtained performing interface sharpening at regular time intervals and using the indicator (18), respectively. Mass correction is automatically switched on when interface sharpening is performed and mass error exceeds the prescribed value 0.2kg. The interface sharpening governed by the indicator (the curve $cuk5M$) better preserves mass at the beginning of computations and in the time interval $t = [0.5; 0.8]$ s. The results obtained by regular interface sharpening (the curve $nsk5M$) are better in the time interval $t = [0.4; 0.5]$ s. Other curves illustrate the modifications of the interface sharpening frequency considering the mass error. The curve $cuk5AM$ illustrates the interface sharpening governed by the indicator and the mass error. The interface sharpening is performed only if it is required by the indicator and the mass error exceeding the prescribed value at the same time step. The logical AND operator is present in the conditional IF statement. The interface is sharpened less frequently (Fig. 8), therefore, mass conservation is not sufficiently improved. The curve $cuk5OM$ is obtained by substituting logical AND to logical OR in the conditional IF statement. The plotted curve demonstrates the obvious improvement in mass conservation. However, the interface sharpening number $shnum$ is considerably increased (Fig. 8), while the efficiency is reduced.

5. Conclusions

In this paper, the development of the efficient interface sharpening procedure for viscous incompressible flows including breaking waves has been described. The dam break problem has been solved by the pseudo-concentration method and the developed interface sharpening technique. The numerical approach has been validated by quantitative

comparison with the experimental measurements. The computed position of the leading edge of the collapsing water column has been in good agreement with the experimental data. The accurate numerical solution of the dam break problem, including highly non-linear breaking waves, proves that the developed interface sharpening technique is capable of recovering interface sharpness and ensuring satisfactory mass conservation. The detailed investigation of numerical parameters has revealed the importance of the interface sharpening frequency for interface thickness as well as for the physics of the flow. The interface sharpening procedure consumes significantly less than 1% of the total computing time, therefore, it can be effectively applied to any complex 3D flows with interfaces undergoing large topological changes.

Acknowledgement

The work is partly supported by the Lithuanian State Science and Studies Foundation in the framework of the project GridTechno (the contract number B-07043). The computational resources provided by the LitGRID (Ministry of Education and Science, ISAK-1570) are also gratefully acknowledged.

References

- Aliabadi, S., and T.E. Tezduyar (2000). Stabilized-finite-element/interface-capturing technique for parallel computation of unsteady flows with interfaces. *Computational Methods in Applied Mechanics and Engineering*, **190**(3–4), 243–261.
- Brackbill, J.U., D.B. Kothe and C. Zemach (1992). A continuum method for modeling surface tension. *J. Computational Physics*, **100**(2), 335–354.
- Čiegis, R., and V. Starikovicius (2003). Realistic performance prediction tool for the parallel block LU factorization algorithm. *Informatica*, **14**(2), 167–180.
- Del Pin, F., S. Idelsohn, E. Oñate and R. Aubry (2007). The ALE/Lagrangian particle finite element method: a new approach to computation of free-surface flows and fluid-object interactions. *Computers & Fluids*, **36**(1), 27–38.
- Grooss, J., and J.S. Hesthaven (2006). A level set discontinuous Galerkin method for free surface flows. *Computer Methods in Applied Mechanics and Engineering*, **195**(25–28), 3406–3429.
- Harlow, F.H., and J.E. Welch (1965). Numerical calculation of time-dependent viscous incompressible flow. *J. Physics of Fluids*, **8**(12), 2182–2189.
- Hirt, C.W., A.A. Amsden and J.L. Cook (1974). An arbitrary Lagrangian-Eulerian computing method for all flow speeds. *J. Computational Physics*, **14**(3), 227–253.
- Hirt, C.W., J.L. Cook and T.D. Butler (1970). A Lagrangian method for calculating the dynamics of an incompressible fluid with free surface. *J. Computational Physics*, **5**(1), 103–124.
- Hirt, C.W., and B.D. Nichols (1981). Volume of fluid (VOF) method for the dynamics of free boundaries. *J. Computational Physics*, **39**(1), 201–225.
- Kačeniauskas, A. (2000). Two-phase flow modelling by the level set method and finite elements. *J. Power Engineering*, **4**, 22–31.
- Kačeniauskas, A. (2004). Parallel GMRES solution of convective transport problems on distributed memory computers. *J. Information Technology and Control*, **30**(1), 69–73.
- Kačeniauskas, A., and P. Rutschmann (2004). Parallel FEM software for CFD problems. *Informatica*, **15**(3), 363–378.
- Kačeniauskas, A. (2005). Dam break flow simulation by the pseudo-concentration method. *J. Mechanika*, **51**(1), 39–43.

- Koshizuka, S., H. Tamako and Y. Oka (1995). A particle method for incompressible viscous flow with fluid fragmentation. *J. Computational Fluid Dynamics*, **4**(1), 29–46.
- Lewis, R.W., and K. Ravindran (2000). Finite element simulation of metal casting. *Int. J. for Methods in Engineering*, **47**(31–3), 29–59.
- Maknickas, A., A. Kačeniauskas, R. Kačianauskas, R. Balevičius and A. Džiugys (2006). Parallel DEM software for simulation of granular media. *Informatica*, **17**(2), 207–224.
- Martin, J.C., and W.J. Moyce (1952). An experimental study of the collapse of liquid columns on a rigid horizontal plane. *Philosophical Transactions of the Royal Society of London, Series A, Mathematical and Physical Sciences*, **244**(882), 312–324.
- Masud, A., and T.J.R. Hughes (1997). A space-time Galerkin/least-squares finite element formulation of the Navier–Stokes equations for moving domain problems. *Computational Methods in Applied Mechanics and Engineering*, **146**(1–2), 91–126.
- Mencinger, J., and I. Žun (2007). On the finite volume discretization of discontinuous body force field on collocated grid: Application to VOF method. *J. Computational Physics*, **221**(2), 524–538.
- Nagrath, S., K.E. Jansen and Jr.R.T. Lahey. Computation of incompressible bubble dynamics with a stabilized finite element level set method. *Computer Methods in Applied Mechanics and Engineering*, **194**(42–44), 4565–4587.
- Nakayama, T., and M. Shibata (1998). A finite element technique combined with gas-liquid two-phase flow for unsteady free surface flow problems. *Computational Mechanics*, **22**(2), 194–202.
- Osher, S., and J.A. Sethian (1988). Fronts propagating with curvature-dependent speed: algorithms based on hamilton-jacobi formulation. *J. Computational Physics*, **79**(1), 12–49.
- Quecedo, M., and M. Pastor (2001). Application of the level set method to the finite element solution of two-phase flows. *Int. J. for Numerical Methods in Engineering*, **50**(3), 645–663.
- Quecedo, M., M. Pastor, M.I. Herreros, J.A.F. Merodo and Q. Zhang (2005). Comparison of two mathematical models for solving the dam break problem using the FEM method. *Computer Methods in Applied Mechanics and Engineering*, **194**(36–38), 3984–4005
- Radovitzky, R., and M. Ortiz (1998). Lagrangian finite element analysis of Newtonian fluid flows. *Int. J. Numerical Methods in Engineering*, **43**(4), 607–619.
- Soulis, J.V. (1992). Computation of two-dimensional dam-break flood flows. *Int. J. for Numerical Methods in Fluids*, **14**(1), 631–664.
- Sussman, M., and E. Fatemi (1999). An efficient, interface preserving level set re-distancing algorithm and its application to interfacial incompressible fluid flow. *SIAM J. Scientific Computations*, **20**(4), 1165–1191.
- Tezduyar, T.E. (2007). Finite elements in fluids: Special methods and enhanced solution techniques. *Computers & Fluids*, **36**(2), 207–223.
- Thompson, E. (1986). Use of pseudo-concentration to follow creeping viscous flow during transient analysis. *Int. J. for Numerical Methods in Fluids*, **7**(2), 749–761.

A. Kačeniauskas – head of the Parallel Computing Laboratory of Vilnius Gediminas Technical University (VGTU), Lithuania. Graduated in applied mathematics from the Vilnius University, Lithuania, in 1995. The MS degree in computer science received from the VGTU in 1996. Doctor thesis “Modelling of viscous incompressible flows and free surfaces by the finite element method” defended and PhD degree received from VGTU in 2000. Research interests comprise parallel and distributed computing, computational fluid dynamics, computational electromagnetics, the finite element method, the discrete element method, free surfaces and moving interfaces.

Efektyvios paviršiaus rekonstrukcijos procedūros, skirtos klampioms nespūdžioms tėkmėms modeliuoti, kūrimas ir tobulinimas

Arnas KAČENIAUSKAS

Straipsnyje aprašomas efektyvios paviršiaus rekonstrukcijos procedūros, taikomos klampioms nespūdžioms dvipusių paviršių tėkmėms modeliuoti, kūrimas ir tobulinimas. Tėkmė nusakoma Navje ir Stokso lygtimis, o kintantis dvipusis paviršius modeliuojamas pseudokoncentracijos metodu. Uždavinio apibrėžimo sritis diskretizuojama erdvės ir laiko baigtiniais elementais, o skaitinės schemos stabilizuojamos Galiorkino mažiausių kvadratų metodu. Skaitinė procedūra ištestuota sprendžiant sugriuvusios užtvankos uždavinį su lūžtančiomis bangomis. Skaitiniais metodais apskaičiuota sklindančio vandens stulpelio krašto padėtis palyginta su eksperimentinių matavimų rezultatais. Pateikta detali skaitinių parametų, reguliuojančių dvipusio paviršiaus glodumą ir tėkmės masės tvermę, studija.